Zooming in REE and Other Trace Elements on Conodonts: Does Taxonomy Guide Diagenesis?

Luca Medici[1], **Martina Savioli**[2], **Annalisa Ferretti***[2], **Daniele Malferrari**[2]

1. *National Research Council of Italy, Institute of Methodologies for Environmental Analysis, C. da S. Loja-Zona Industriale, 85050 Tito Scalo, Potenza, Italy*
2. *Department of Chemical and Geological Sciences, University of Modena and Reggio Emilia, Via Campi 103, 41125 Modena, Italy*

Luca Medici: https://orcid.org/0000-0001-9426-4653; Martina Savioli: https://orcid.org/0000-0001-6358-4320; Annalisa Ferretti: https://orcid.org/0000-0002-1173-8778; Daniele Malferrari: https://orcid.org/0000-0002-0879-1703

ABSTRACT: Conodont elements are calcium phosphate (apatite structure) mineralized remains of the cephalic feeding apparatus of an extinct marine organism. Due to the high affinity of apatite for rare earth elements (REE) and other high field strength elements (HFSE), conodont elements were frequently assumed to be a reliable archive of sea-water composition and changes that had occurred during diagenesis. Likewise, the crystallinity index of bioapatite, i.e., the rate of crystallinity of biologically mediated apatite, should be generally linearly dependent on diagenetic alteration as the greater (and longer) the pressure and temperature to which a crystal is exposed, the greater the resulting crystallinity. In this study, we detected the uptake of HFSE in conodont elements recovered from a single stratigraphic horizon in the Upper Ordovician of Normandy (France). Assuming therefore that all the specimens have undergone an identical diagenetic history, we have assessed whether conodont taxonomy (and morphology) impacts HFSE uptake and crystallinity index. We found that all conodont elements are characterized by a clear diagenetic signature, with minor but significant differences among taxa. These distinctions are evidenced also by the crystallinity index values which show positive correlations with some elements and, accordingly, with diagenesis; however, correlations with the crystallinity index strongly depend on the method adopted for its calculation.
KEY WORDS: bioapatite, crystallinity index, HFSE, laser ablation, mass spectrometry, microdiffraction, Normandy, Ordovician.

0 INTRODUCTION

Conodont elements are the mineralized remains of the cephalic feeding apparatus of an extinct marine organism whose taxonomic attribution has been strongly debated in the past before being finally assessed among Vertebrates (see Sweet and Donoghue, 2001 for a review). Conodonts lived in the ancient oceans for over 300 Ma from the Cambrian to the Triassic/Jurassic transition. Thanks to their rapid evolution and diversity of habitats, conodonts represent a fundamental tool for biostratigraphic assignments and a valuable aid in paleogeographic reconstructions (Ferretti et al., 2020a). Elements, organized in apparatuses, reveal an extreme morphological inter- and intra-apparatus variability, but with elements sharing two main phosphatic and crystallized parts: (i) a basal body, rarely preserved and characterized by a low to medium tissue density; (ii) a hyaline and an albid crown, both variably distributed within cusps and denticles and characterized

by a medium (hyaline) to high (albid) tissue density (e.g., Li et al., 2017; Zhao et al., 2013; Trotter et al., 2007; Trotter and Eggins, 2006).

Conodonts are constituted by bioapatite, a name generally used to indicate an apatite of strictly biochemical origin. The chemical formula usually assigned to bioapatite is $Ca_5(PO_4,CO_3)_3(F,OH)$. According to the amount of substitutions in the anionic sites, bioapatite was also referred in the past with different mineral names (e.g., francolite, dahllite) which, however, have been now discredited by the Commission on New Minerals and Mineral Names (CNMMN). In spite of these formal aspects, a certainty remains: different iso- and hetero-valent substitutions occur in the bioapatite framework both in the anionic and cationic sites (LeGeros, 1981). The cationic replacements can be relevant or minor, with Ca respectively substituted by major elements (mostly Na and Mg; e.g., Keenan and Engel, 2017; Keenan, 2016; Brigatti et al., 2004) or by REE and other trace elements (e.g., Li et al., 2017; Zhao et al., 2013; Trotter et al., 2007; Trotter and Eggins, 2006; Trueman and Tuross, 2002; Reynard et al., 1999; Grandjean-Lécuyer et al., 1993).

The replacing cations are incorporated during *in-vivo* biologically-mediated crystal growth or during *post-mortem* bur-

ial and diagenesis. In the past, content of rare earth elements (REE) and trace elements (mostly others high field strength elements, HFSE) in fossil bioapatite was generally assumed to be a reliable archive of sea-water composition (e.g., Song et al., 2019; Pietsch and Bottjer, 2010; Girard and Albarède, 1996; Grandjean-Lécuyer et al., 1993; Grandjean et al., 1987; Wright et al., 1984). However, as early as the 1990s, concrete hypotheses began to be advanced in which HFSE concentration in bioapatite could have been considerably affected by other parameters (Picard et al., 2002; Armstrong et al., 2001; Reynard et al., 1999; Holser, 1997; Toyoda and Tokonami, 1990), generally triggered by the geochemistry (i.e., overall chemical and mineralogical composition) of the diagenetic environment (Žigaitė et al., 2020; Liao et al., 2019; Trotter et al., 2016; Zhang et al., 2016; Chen et al., 2015; Herwartz et al., 2013, 2011; Zhao et al., 2013; Kocsis et al., 2010; Trotter and Eggins, 2006). Although there is still no unanimous agreement (Liao et al., 2019), the hypothesis of a diagenetic imprint is undoubtedly more likely (Trotter et al., 2016; Zhang et al., 2016; Chen et al., 2015; Kim et al., 2012; Lécuyer et al., 2004), and Zhang et al. (2016) even suggested that all researches in which bioapatite has been considered as a proxy being based exclusively on HFSE concentration and REE anomalies should be reviewed.

Bioapatite may record a REE signature from sea-water (hydrogenous signature) which is usually characterized by low ΣREE (sum of all REEs content) and marked LREE (light REEs, i.e., La, Ce) deficit (Webb et al., 2009; Lécuyer et al., 2004; Nothdurft et al., 2004; Webb and Kamber, 2000; Grandjean-Lécuyer et al., 1993; Wright et al., 1987). Later, in the burial environment, the uptake of REE will be controlled by diagenesis which imparts a signature (pore-water signature) several orders higher than the hydrogenous one (Zhang et al., 2016; Chen et al., 2015; Pattan et al., 2005). Reliable information on the hydrogenous signature is provided by Y/Ho as, in modern ocean water, Ho is adsorbed or complexed at about twice the rate of Y (Xin et al., 2016; Nozaki et al., 1997; Zhang and Nozaki, 1996; Zhang et al., 1994), generating a Y/Ho ratio for sea-water about twice that of terrigenous materials (McLennan, 2001). Therefore, higher Y/Ho represents a larger fraction of sea-water derived (hydrogenous) REE, and lower Y/Ho indicates a larger fraction of terrigenous derived (lithogenous) REE. On the other hand, the pore-water signature is usually marked by high ΣREE and strong Th and LREE enrichment (a lithogenous signal mainly from clay minerals; Shen et al., 2012; Peppe and Reiners, 2007; McLennan, 2001; Wright and Colling, 1995) and, more rarely by MREE (middle REEs, i.e., Pr, Nd, Sm, Eu) and HREE (heavy REEs, i.e., Gd, Tb, Dy, Ho, Er, Tm, Yb, Lu) enrichments related to an authigenic phosphate signal (Bright et al., 2009; Reynard et al., 1999; Sholkovitz and Shen, 1995). Actually, a rapid assessment of REE sources can be made on the basis of Th vs. ΣREE and Y/Ho vs. ΣREE cross-plots (Li et al., 2017).

In addition to HFSE, another parameter that can be related to the degree of diagenesis is the crystallinity index (CI), although applied less frequently and sometimes leading to questionable results (Trueman et al., 2008; Pucéat et al., 2004). The CI is a measure of the structural order within crystals. Several methods for CI assessment are described in the literature (e.g., Pucéat et al., 2004; Person et al., 1995), all generally based on

the shape and intensity of selected X-ray powder diffraction peaks which mainly depend on crystal size, structural order, texture and amount/type of iso- and hetero-valent major substitutions. The correlation between CI and diagenesis should be that the greater (and longer) the pressure and temperature to which a crystal is exposed, the greater the resulting crystallinity. In fact, during *in-vivo* biologically-mediated crystal growth, bioapatite crystallites are intimately associated and intergrown with the organic matrix. After death, the organic phase is more or less rapidly decomposed and the inorganic phosphate crystals may be re-arranged and distributed in the empty spaces. This structural and textural re-organization should generally imply an increase of CI (Trueman et al., 2008). At the same time, the breakdown of the organic component also enhances the diffusion of water (Collins et al., 2002) and, consequently, increases as well the rate and amount of exchange/adsorption reactions occurring at the solid/water interface. It is reasonable to expect, therefore, that high CI values should pair high ΣREE, LREE, Th concentrations and, conversely, low CI values couple low ΣREE, marked LREE deficit and high Y/Ho ratio. Literature reports several evidences that the ultrastructure of bioapatite, which is strongly related to CI, plays a relevant role in HFSE uptake rate and extension (Kohn and Moses, 2013; Herwartz et al., 2011; Trueman et al., 2008; Pucéat et al., 2004; Trueman and Tuross, 2002; Toyoda and Tokonami, 1990), but rarely (Žigaitė et al., 2020) focusing on conodont taxonomy and/or element morphology.

In this study, we detected the uptake of HFSE in conodont elements from the Upper Ordovician of Normandy ("Vaux Limestone", outcropped close to the village of Saint-Hilaire-la-Gérard). Assuming that the material has undergone an identical diagenetic history (specimens come from the same stratigraphic horizon), we have assessed whether conodont taxonomy and element morphology impacts HFSE uptake. We then compared resulting data with CI values previously detected exactly in the same positions where the chemical measurements were collected.

1 MATERIALS AND METHODS
1.1 Samples and Sample Preparation
Material investigated in this study was collected in Normandy (NW France) and described by Ferretti et al. (2014c), who sampled in 2006 and 2007 the locality reported by Weyant et al. (1977) located about 2 km SW of Saint-Hilaire-la-Gérard in the Sées syncline (Fig. 1). The area hosts nowadays the Normandie-Maine Regional Natural Park, a protected area that will preserve the outcrop for the future. Ferretti et al. (2014c) tried to test the paleogeographic affinity of the Late Ordovician conodont fauna from Normandy, a geographic sector located aside Brittany (e.g., Paris et al., 1981; Lindström and Pelhate, 1971) in a key-position between the British Isles (for updated conodont references see Bergström and Ferretti, 2015; Ferretti et al., 2014a, b), Baltoscandia (e.g., Dzik, 2020, 1999, and references therein) and Continental Europe (see, among others, Del Moral and Sarmiento, 2008; Ferretti and Schönlaub, 2001; Ferretti and Serpagli, 1999, 1991; Ferretti and Barnes, 1997).

A total of 90 kg of limestone was processed in formic acid using standard methods of conodont extraction. The conodont association described by Ferretti et al. (2014c) was assigned to

the middle Katian and resulted dominated by *Amorphognathus* and *Scabbardella*, with *Sagittodontina* and *Hamarodus* common as well. Just the presence of the latter, concentrated in some levels, is significant as the genus is absent from Brittany. The authors confirmed the *Sagittodontina robusta-Scabbardella altipes* biofacies already proposed by Sweet and Bergström (1984).

Among this material, we selected specimens of the three main documented genera (Fig. 2): *Sagittodontina* (one specimen; P element), *Scabbardella* (two elements) and *Amorphognathus* (six elements: two Pa elements, two Pb elements, one Sb element and one Sc element). All these elements were collected from the same stratigraphic horizon and, more specifically, from the same sample (level W2).

All analysed material is housed in the Paleontological Collections of the University of Modena and Reggio Emilia: under accession prefix IPUM at the Department of Chemical and Geological Sciences, University of Modena and Reggio Emilia, Modena, Italy.

1.2 Instruments and Analytical Methods
1.2.1 Chemical measurements

Tuning the ablation parameters is of paramount relevance in this kind of studies as their value strictly rules the quantity of material (i.e., bioapatite) removed by the laser beam. The various mineralized tissues react differently to the laser impulses (Malferrari et al., 2019) and the amount of ablated bioapatite depends on crystallites density, crystals size and morphology, overall chemical composition and sample shape. Nevertheless, it is not even possible to know *a priori* the point-by-point re-

sponse of the sample to the laser impulses so to fine-tune the ablation parameters accordingly. This issue is further amplified by the lack of a true matrix-matched (composition and hardness) calibration standard for LA-ICPMS measurements on fossil bioapatite. The NIST SRM 1400 Bone Ash and NIST SRM 1486 Bone Meal could represent possible compromise, even if they are specifically designed to prepare liquid standard solutions and, moreover, have concentrations of most trace elements considerably lower than those usually found in fossils. Hence, the NIST SRM 610 and NIST SRM 612, despite their silica-glass matrix, have often been preferred, mediating through the development of opportune calibration strategies and discussing element ratios, or other relationships, rather than elements absolute concentrations.

Here we adopted a calibration strategy encompassing both silica and phosphatic standards and using the ICP-MS X Series II (Thermo Fisher Scientific) equipped with the 213 nm laser ablation device UP-213 (New Wave Research). Prior to optimizing laser ablation parameters for the conodont elements, the instrument was tuned using the NIST SRM 610 and NIST SRM 612 glasses measuring, at instrument-optimized working conditions, the intensity of the signals from U and Th (U/Th *vs.* U). Later, according to methods already adopted in past researches (e.g., Ferretti et al., 2020b; Malferrari et al., 2019; Nardelli et al., 2016), we prepared a pressed tablet with the NIST SRM 1400 and, using the NIST SRM 610 and NIST SRM 612 as calibrating standards, we modulated the ablation parameters up to gain for NIST SRM 1400 tablet (considered as unknown sample) the concentrations of selected trace elements which amount in NIST SRM 1400 is
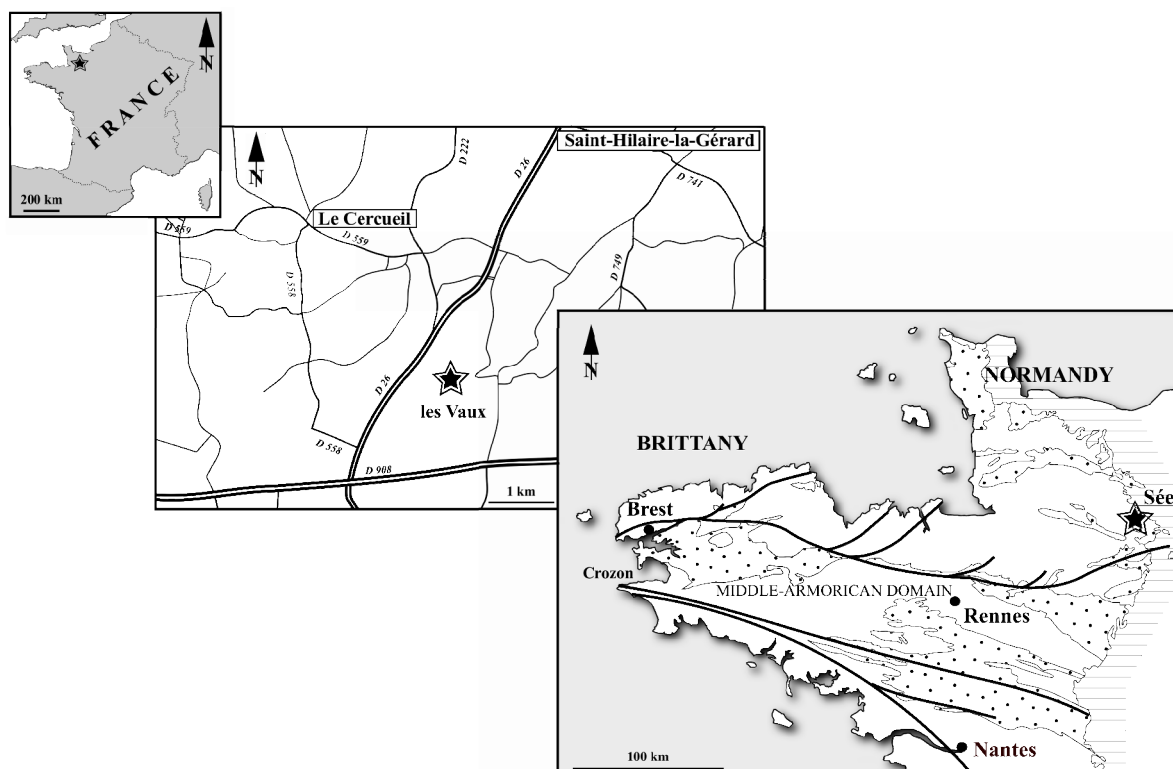
Figure 1. Geographical and geological maps of the sampling area located about 2 km SW of Saint-Hilaire-la-Gérard in the Sées syncline. The outcrop is now part of the Normandie-Maine Regional Natural Park (48°35'14"N, 0°02'33"E). Modified after Vidal et al. (2011) and Ferretti et al. (2014c). Stippling indicates Paleozoic units, horizontal lines represent Mesozoic units, white refers to Proterozoic and Cadomian units and to igneous Variscan units.

Figure 2. Selected specimens (after laser ablation) of the three main genera documented in the "Vaux Limestone", Late Ordovician, Normandy. (1), (2) *Scabbardella altipes* (Henningsmoen, 1948), lateral views of elements IPUM 29850 and IPUM 29851, respectively. (3), (4) *Amorphognathus* sp., upper view of Pa element IPUM 29852 and lateral view of Sb element IPUM 29853, respectively. (5) *Sagittodontina robusta* Knüpfer, 1967, lateral view of P element IPUM 29854. Frames illustrate details of selected ablated areas. Scale bars correspond to 100 μm.

bracketed by (i.e., Sr and K) or close to (i.e., Fe, Mn, Pb and Zn) those of NIST SRM 612 and NIST SRM 1400. The obtained optimized ablation parameters (Table S1) were later applied to standards (NIST SRM 610 and NIST SRM 612) and samples (conodont elements). However, as already pointed out by Zhang et al. (2017), this method leaves unsolved the lack of a univocal internal standard as Ca and/or P (the most used references) in conodonts can vary significantly for isomorphic substitutions.

Another thing to carefully consider is the type of tissue to be analyzed. Various authors (e.g., Trotter et al., 2016; Zhang et al., 2016; Frank-Kamenetskaya et al., 2014; Zhao et al., 2013;

Wheeley et al., 2012; Trotter and Eggins, 2006) reported that the albid tissue, in view of its high hardness and low porosity, is usually better and more frequently preserved and, in comparison mostly to the basal body (or basal cavity), it is less affected by chemical contamination from detrital residues (Trotter et al., 2007; Wenzel et al., 2000; Holmden et al., 1996). Nevertheless, Zhang et al. (2017) observed that the albid and hyaline crowns are more affected by recrystallization (as proxied by the sharp of X-ray diffraction peaks) rather than the basal body; consequently, they concluded that the practice of selectively utilizing the albid crown for geochemical studies of conodonts should be

carefully re-evaluated.

We agree that, in comparing absolute concentrations of HFSE in conodonts from different geographic areas, it is crucial to take the measurements always on the same type of tissue, so to reduce the number of variables. On the other hand, when comparing and correlating the HFSE uptake among conodont elements within the same fauna, average values between diverse tissues are probably preferable, especially whether high CAI may prevent a clear tissue distinction. For the same reason, we processed our material by small ablation lines (Table S1) rather than points in order to gain more signal to integrate and, consequently, mitigate any density anomalies.

1.2.2 X-ray microdiffraction (μ-XRD)

The μ-XRD measurements (described below) used to calculate CI were collected in the same element areas which were later ablated and chemically characterized. The analytical technique and the instrument are already described in the literature (e.g., Medici et al., 2020; Ferretti et al., 2017). The experimental conditions here applied are reported in Table S1. The crystallinity index values were calculated following three different procedures.

The first one, referred as CI-M1, was primary described by Person et al. (1995) and later refined by Pucéat et al. (2004) to determine the degree of chemical alteration of biogenic apatite. The CI value is calculated considering the heights H, where $H[211]$ is the height of the (211) reflection, $H[112]$ $H[300]$ $H[202]$ represent the difference between the top of the peak and the value of the minimum separating it from the previous peak, for the (112), (300), (202) reflections, respectively. The formula can be summarized as $CI = \Sigma\{H[202], H[300], H[112]\}/H[211]$.

The second index (CI-M2), is more commonly employed in crystallography and considers the full width at half maximum (FWHM), which is the width of an XRD peak measured between those two points (2θ) that are at half of the maximum intensity of the peak. This method is sensitive to the variation in microstructure and stress/strain accumulation in the material and it is inversely correlated to the degree of crystallinity. It is

usually calculated as the sum (e.g., Zhang et al., 2017) or the average (this study) of the values measured for some selected reflections—here we considered the (300), (222), (132) and (321) as they are better defined in all the nine elements studied.

Both methods are indicative of the crystallinity rate. The main difference is that the former allows direct comparison also with measurements from previous studies (although so far absent for conodonts), while the latter is strictly dependent on the instrument and on the applied experimental conditions.

The crystallinity index by Person et al. (1995) refers to data obtained by powdered samples; on the contrary, here X-ray microdiffraction data were measured in specific areas of the samples (i.e., those after chemically characterized) without any pre-treatment. Therefore, measurements could be affected by the morphologies of the elements and by crystal preferential orientations which could underestimate the intensity of the (211) reflection (Medici et al., 2020). In the light of these considerations, a third crystallinity index (CI-M3) is proposed in this paper as a modification of CI-M1 index. It is calculated as $CI = \Sigma\{H_1, H_2, H_3\}/H_M$, where H_M corresponds to the highest value among $H[211]$, $H[112]$, $H[300]$, and $H[202]$ in CI-M1 crystallinity index by Person et al. (1995) and H_1, H_2, and H_3 represent the other three values.

2 RESULTS

A list of statistically significant relationships among HFSE is reported in Table 1, whereas chemical analyses and normalized concentrations (McLennan, 2001) are given in Table S2.

All the samples are characterized by a substantial enrichment of MREE and HREE as shown by the lower $(La/Sm)_N$ and $(La/Yb)_N$ ratios (Table 1, Fig. S1). Distribution of UCC-normalized (McLennan, 2001) REE (Fig. 3) outlines two patterns which pair *Scabbardella* (Sc) and *Sagittodontina* (Sa) on one side (type I) and the elements (Pa, Pb, Sb and Sc) of *Amorphognathus* (Am) on the other (type II). This distinct behavior is expressed also by the linear distribution of Y *vs.* La, Nd and Yb considered as representative of LREE, MREE and HREE, respectively (Figs. 4, S2) and by the MREE anomaly (MR/MR*, Table 1), i.e., the
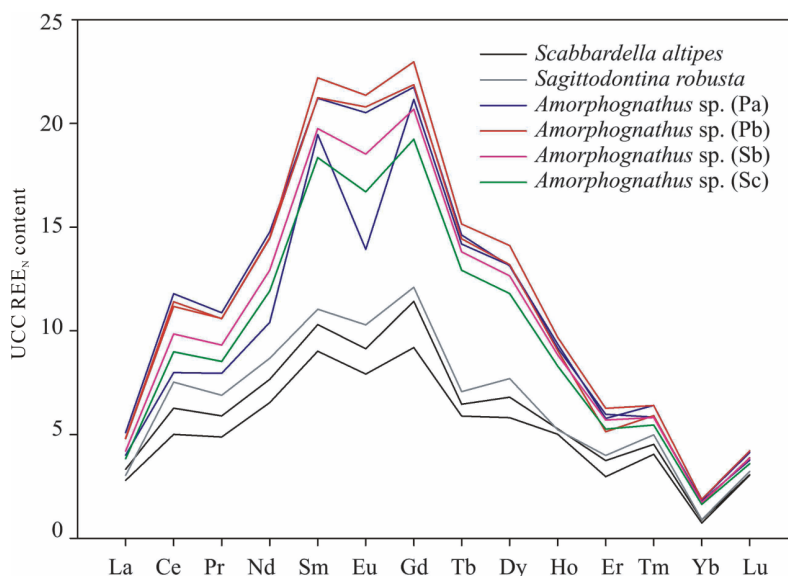

Figure 3. UCC normalized (McLennan, 2001) REE abundance patterns for conodont elements.

Table 1 Statistically significant relationships among HFSE. Sums of REE are in ppm.

	CI-M1	CI-M2	CI-M3	La/Y	La/Yb	Y/Ho	MR/MR*	Pr/Pr*	Ce/Ce*	Gd/Gd*	Eu/Eu*
Scabbardella altipes	1.911	0.243	0.552	0.759	51.71	27.48	0.596	0.845	1.241	1.331	0.870
Scabbardella altipes	1.447	0.265	0.738	0.835	51.82	28.31	0.565	0.846	1.314	1.465	0.841
Sagittodontina robusta	0.880	0.240	0.880	0.734	46.04	29.64	0.559	0.851	1.532	1.396	0.889
Amorphognathus sp. (Pa)	0.921	0.260	0.921	0.803	38.63	25.92	0.606	0.818	1.418	1.238	0.955
Amorphognathus sp. (Pa)	0.874	0.219	0.874	0.641	29.25	25.03	0.635	0.864	1.300	1.505	0.686
Amorphognathus sp. (Pb)	1.063	0.219	1.063	0.727	34.78	25.55	0.632	0.825	1.391	1.258	0.946
Amorphognathus sp. (Pb)	0.982	0.257	0.982	0.775	39.08	25.83	0.617	0.818	1.418	1.241	0.965
Amorphognathus sp. (Sb)	2.379	0.217	0.457	0.700	33.25	25.46	0.638	0.818	1.385	1.279	0.916
Amorphognathus sp. (Sc)	4.864	0.213	0.221	0.680	32.03	25.45	0.643	0.815	1.376	1.299	0.889

	(La/Sm)$_N$	(La/Yb)$_N$	HR/LR	(La+Th)	ΣLREE	ΣMREE	ΣHREE	ΣREE	ΣREE/Th	log (ΣREE)	log (ΣREE/Th)
Scabbardella altipes	0.309	3.792	0.183	104	404	252	74	730	36.51	2.863	1.562
Scabbardella altipes	0.323	3.800	0.177	122	501	295	89	885	39.60	2.947	1.598
Sagittodontina robusta	0.275	3.376	0.167	157	572	333	95	1 001	15.18	3.000	1.181
Amorphognathus sp. (Pa)	0.240	2.833	0.183	186	907	575	166	1 648	49.91	3.217	1.698
Amorphognathus sp. (Pa)	0.206	2.145	0.260	201	631	427	164	1 222	15.16	3.087	1.181
Amorphognathus sp. (Pb)	0.216	2.551	0.205	192	859	571	176	1 606	33.81	3.206	1.529
Amorphognathus sp. (Pb)	0.228	2.866	0.188	181	875	565	164	1 604	44.45	3.205	1.648
Amorphognathus sp. (Sb)	0.213	2.438	0.210	175	756	507	159	1 422	28.91	3.153	1.461
Amorphognathus sp. (Sc)	0.209	2.349	0.214	164	690	468	148	1 306	26.43	3.116	1.422

ratio of the observed to the expected concentration of MREE here is calculated as suggested in Chen et al. (2015). Likewise, similar observations are provided by the crossplots (Fig. S3) of La_N *vs.* Pr_N (i.e., LREE/LREE), La_N *vs.* Gd_N (i.e., LREE/MREE), and La_N *vs.* Yb_N (i.e., LREE/HREE). Ce/Ce* and Eu/Eu* values (here calculated as Ce/Ce*=$3Ce_N$/($2La_N+Nd_N$) and Eu/Eu*= $2Eu_N$/(Sm_N+Gd_N), respectively (Shields and Stille, 2001), which mirror the reducing/oxidizing conditions of the burial environment, are relatively consistent (Table 1) and are not clustered, suggesting that the redox environment equally imprints each type of conodont. Eu/Eu* is characterized by values ranging from 0.69 to 0.97 (the average value is 0.88), which indicates a clearly negative Eu anomaly. The Ce/Ce* *vs.* Pr/Pr* plot (Fig. S4), where Pr/Pr*=$2Pr_N$/(Ce_N+Nd_N), confirms the positive Ce anomaly for all the samples basing on the model from Kowal-Linka et al. (2014).

The (La+Th) and ΣREE *vs.* Y/Ho cross plots may be used to evaluate the REE contribution of terrigenous material as in terrigenous sediments REE and Th are high in concentration, while Y and Ho are more prevalent in sea-water. All the samples show Y/Ho ratios between 25 and 30 (Table 1), clearly indicative of a strong diagenetic contribution, however once again highlighting the distinction between type I and type II (that is *Sagittodontina* and *Scabbardella* on one side, and *Amorphognathus* on the other, Fig. S5). The marked imprint of diagenesis as well as the diversification between the two clusters is here further evidenced by the positive correlations between Y and ΣREE or U (Fig. S6) and by the inverse correlation between Y/Ho and MR/MR* (Fig. S7), whereas less meaningful are the correlations between Y and Th.

Sr is not correlated systematically with any other elements

including REE. Although Sr may be taken up *in vivo* (Trotter and Eggins, 2006), high Sr concentrations in fossil apatite usually mirror its solubility in sediment pore-waters and long-term uptake in the burial environment (Martin and Scher, 2004; Holmden et al., 1996).

As far as crystallinity concerns, a relevant relationship, once again highlighting the double clustering evidenced by chemical analyses, was found between ΣHREE and CI-M3 (Fig. 5a). Less significant correlations were found also between log (ΣREE/Th) and 1/(CI-M1) and between La/Y and CI-M2 (Figs. 5b, 5c, respectively), but in this case without paralleling the clustering described above.
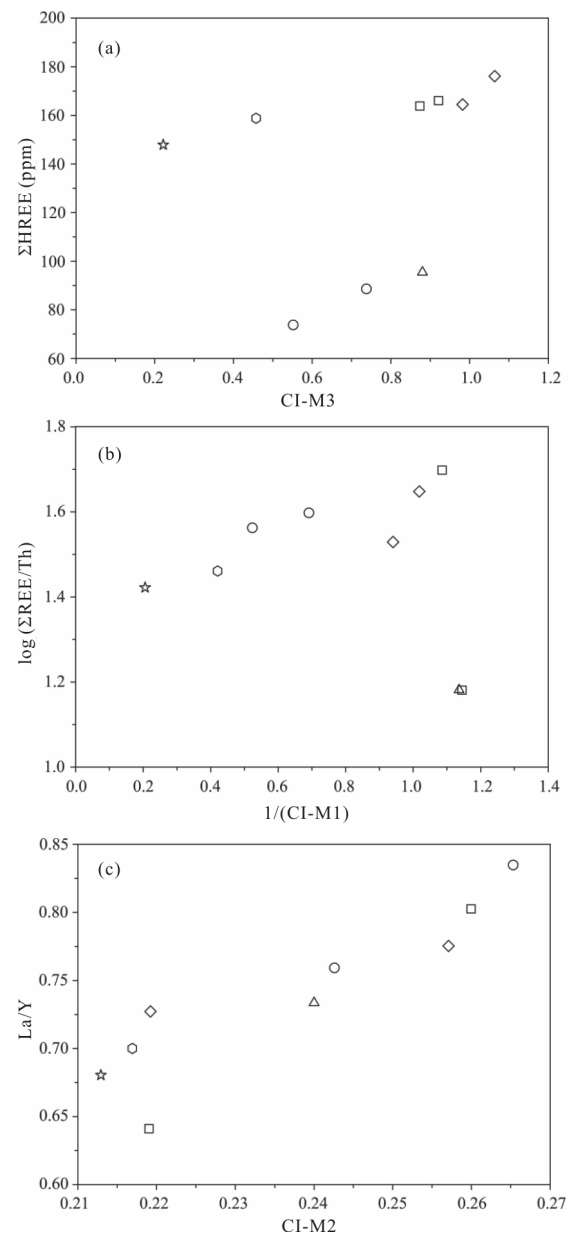
3　DISCUSSION

The origin of HFSE incorporated in fossils is not easily constrained. As mentioned in the INTRODUCTION, the HFSE composition of bioapatite has long been used for reconstruction of paleoceanographic conditions based on the shape of normalized REE distributions, REE anomalies and correlation between REE and/or other trace elements. On the other hand, several evidences suggested that also the hydrogenous signal present in fossils could be critically affected by diagenetic overprints. In our samples, diagenesis leads to an increase in the total REE content (Table S2) associated with low Y/Ho ratios (Fig. S5). This result indicates that the REE budget is dominantly derived from the pore-waters of the embedding sediments, as confirmed also by the concomitant increase of U and, in less amount, of Th.

Bright et al. (2009) observed that most of the shale-normalized REE patterns in conodonts is characterized by MREE enrichment, although quantitatively variable among samples. The MREE enrichment, even if peaking to Gd (here assigned to
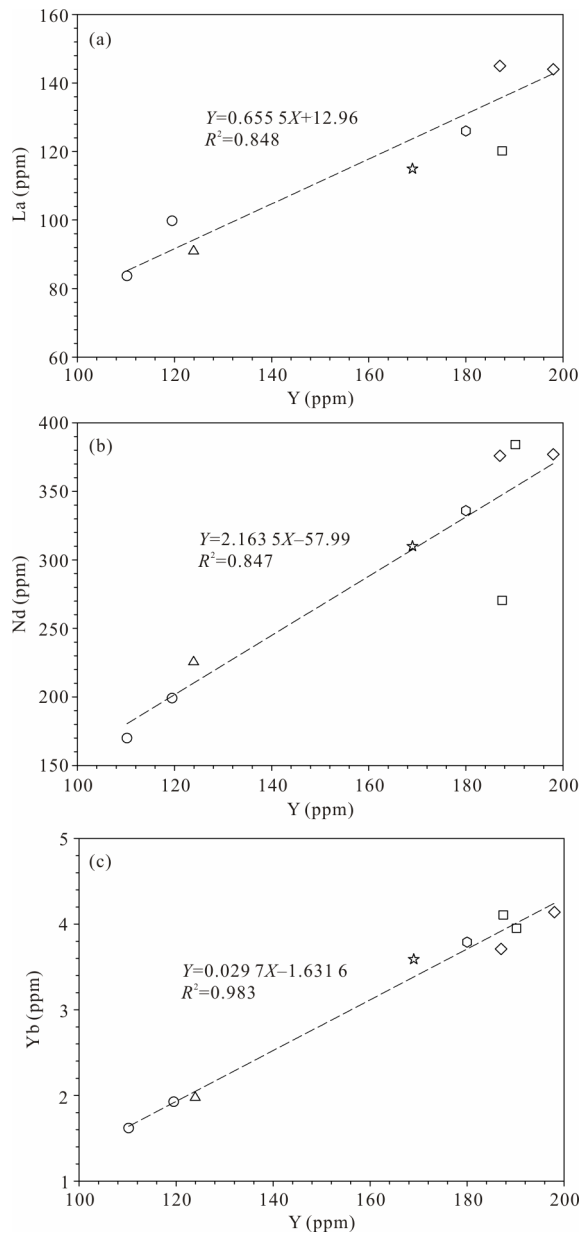
Figure 4. Crossplots of La, Nd, Yb *vs.* Y showing the distribution between types I and II clusters. Symbols: *Scabbardella altipes*, circles; *Sagittodontina robusta*, triangles; *Amorphognathus* sp. (Pa), squares; *Amorphognathus* sp. (Pb), diamonds; *Amorphognathus* sp. (Sb), exagons; *Amorphognathus* sp. (Sc), stars. Dashed lines indicate the linear regression plots (equations and R^2 are reported on the plot).

Figure 5. Diagrams showing the correlations of (a) ΣHREE *vs.* CI-M3; (b) [log (ΣREE/Th)] *vs.* 1/(CI-M1); (c) La/Y *vs.* CI-M2. Symbols are the same as in Fig. 4.

HREE), is well evident also in our samples (bulge pattern, Fig. 3), but with a clear distinction between *Scabbardella* (Sc) and *Sagittodontina* (Sa) on one side (type I) and the elements (Pa, Pb, Sb and Sc) of *Amorphognathus* (Am) on the other (type II). Although this diversification does not question the marked diagenetic imprint for all the samples as proved by the linear correlation between ΣMREE and ΣREE (Fig. S8), it enhances that the REE enrichment deeply marks some taxa rather than others. Such questions arise from several observation, especially as all specimens realistically underwent an identical diagenetic imprint being collected from the same sample. Taxonomy, although minimally, appears to control the degree of chemical fractionation which, therefore, depends not only on the effective

diffusion coefficient, but also on the size of the exposed surface that, due to the small dimensions of conodont elements, otherwise would be reasonably assumed as a negligible parameter.

Various hypotheses have been proposed for several years to explain the MREE enrichment in Paleozoic bioapatite; most of them are mainly ascribable to two main hypotheses: (i) a real seawater MREE enrichment due to a combination of biological and chemical processes which caused a selective uptake and cycling of REE from sea water (e.g., Picard et al., 2002; Girard and Albarède, 1996; Grandjean-Lécuyer et al., 1993); (ii) MREE enrichment resulting from preferential substitution of MREEs for Ca^{2+} in both biogenic and authigenic apatite lattice during diagenetic recrystallization likely masking or delating the original signals (e.g., Trotter and Eggins, 2006; Shields and Webb, 2004; Cruse and Lyons, 2000; Reynard et al., 1999;

McArthur and Walsh, 1984). The latter hypothesis is definitely more accepted (see INTRODUCTION); however, it leaves open the debate about the timing of the enrichment. Our data do not more favorably support one hypothesis or the other as the differentiation we have detected could be linked to both original enrichment as well as diagenesis. Nevertheless, as mentioned above, the linear correlation between MREE and ΣREE (Fig. S8) better supports the diagenetic-dependent imprint. But other than that, very rarely differences in REE concentration among different taxa have been critically zoomed once assessed the diagenetic imprint. To the best of our knowledge, only Bright et al. (2009), comparing MREE concentration in Carboniferous *Idiognathodus* and *Gondolella*, highlighted slight but significant distinctions, however reporting differences less marked compared to ours. As *Idiognathodus* is found both in limestones and shales while *Gondolella* is almost exclusively recovered from phosphatic black shale facies of cyclothems (Heckel and Baesemann, 1975), the resulting differences were associated to the living environment without considering the possible contribution of taxonomy.

Here, in addition to the geochemical markers, we considered also the crystallographic signature. Undoubtedly, the main result is that the double clustering (i.e., types I and II) is paralleled also by the relationship between CI-M3 and ΣHREE, thus suggesting a possible "chemical and structural control" by diagenesis strictly mediated by taxonomy (Fig. 5a). The lack of clustering shown in Figs. 5b–5c suggests that CI-M1 and CI-M2 indexes are not suited for not-powered samples as crystallites could not be randomly distributed, but affected by preferential orientation according to their morphologies (Medici et al., 2020).

Nevertheless, the lack of marked positive correlation between CI and ΣHREE (or, conversely, the lack of an inverse correlation with ΣLREE) can suggest that diagenesis drives crystallinity only up to a "threshold of saturation" as already observed by Pucéat et al. (2004) in fossil biogenic apatites. In the incipient diagenesis the HFSE uptake is mainly controlled by the decomposition of the organic phase and, consequently, by the progressive exposure of the specimen to pore water (Trueman et al., 2008). During burial, CI increases mainly as a response to crystallization of the amorphous part and, in consequence, authigenic apatite crystals grow replicating the unit cell signature of primary bioapatite (Ferretti et al., 2017). In late diagenesis, CI may not significantly increase as the crystal lattice is already formed; at this stage the primary amorphous component is exhausted (i.e., it is crystallized) and the site-specific geochemical conditions become the dominant parameter in controlling chemical substitutions (major and trace elements) at the solid/pore-water interface. At this time the HFSE uptake is no longer limited, breaking down its relationship with CI. Moreover, it should be considered that new authigenic apatite crystals, replicating the original unit cell parameters, are sometimes recognizable only through diffractometric techniques and may form not only in the empty space, but also on the surface (Sanz-López and Blanco-Ferrera, 2012); actually, no significant differences in unit cell parameters were documented between the newly formed apatite crystals and those of the pristine conodont surfaces (Ferretti et al., 2017).

By matching the literature data and those analyzed in this study, a two-step mechanism can be hypothesized.

(1) A *post-mortem* phase in which diffusion of pore-water in the space previously occupied by organic matter occurs simultaneously with a deep recrystallization (Smith et al., 2005; Trueman and Tuross, 2002). This would explain also why the hardest and yet well-crystalized tissues (i.e., albid and hyaline crowns) are less affected by trace element enrichment (Trotter et al., 2016; Zhang et al., 2016; Zhao et al., 2013; Trotter and Eggins, 2006).

(2) A burial and late diagenesis stage in which the pristine bioapatite gets fully recrystallized, but the geochemical imprint goes on. It is in this latter stage that taxonomy appears to play its role, even if the mechanism is still unknown.

The substitutions of REE for Ca^{2+} in original (but organic-free) bioapatite crystal lattice (*post-mortem* phase) are likely several orders of magnitude lower than partition coefficients for REE between pore waters and new apatite crystals (burial and late diagenesis stage). Precipitation of secondary apatite will thus increase the total volume of phosphate mineral, but will not necessarily increase the concentration of REE within the original bioapatite, breaking down the relationship between crystal size and diagenetic trace element content.

In addition to the different partition coefficient of REE between biogenic and authigenic apatite, Trueman et al. (2008) have found that also the rate of closure of intra-crystalline porosity plays a crucial role as it modulates the interactions at the solid/pore-water interface and, therefore, the uptake of REE. The rate of closure of intra-crystalline porosity, which is also a condition for preservation of fossil into deep time, is a multi-parameters dependent factor and it is quite likely that it depends not only on the fossilization and burial environment, but also on the biogenic and taxa-related conformation of the living organism. Although further investigations are needed to provide an experimental demonstration, it is hard to disengage the rate of changing in porosity from geochemical alteration and, therefore, from the loss of a predictive relationship between crystallinity and trace element accumulation.

4   CONCLUSIONS

The Late Ordovician conodont material investigated in this study is undoubtedly characterized by a diagenetic signature, however with minor but significant distinctions among taxa. Differences like these are not relevant for burial environmental interpretations when all the chemical markers converge towards a model of diagenetic enrichment; in contrast, the diagenetic setting can be hardly framed when chemical markers assume values close to the limit typical of the hydrogenous or diagenetic enrichment. How this process develops, and the reasons for this, needs further investigation.

Other matters of critical importance concern crystallinity. The calculation method of the CI, rarely used in paleontological research, should be carefully considered as it strongly depends on sample preparation and textures, the latter mostly when measurements are not taken on powder. In fact, powder provides an average result which may fail in predicting the true rate of geochemical alteration when it is achieved mainly through the growth of authigenic apatite, as a powder diffraction pattern cannot distinguish between the relative proportion of biogenic and authigenic apatite. Actually, the modified crys-

tallinity index CI-M3, which accounts of the effects of preferential orientations (in turn possibly dependent on taxonomy) prove to directly relate with ΣHREE which, in contrast to crystal index, is a well-known and used diagenetic marker.

Regardless of the calculation method, the recrystallization rate of porous and amorphous tissues (basal body) is probably different from that of the hard ones (albid and hyaline crowns), suggesting that the CI "threshold" could be reached first from one tissue rather than the other. Likewise, authigenic crystals grown from solution circulating within a metasomatic environment differs from recrystallization, that is more typical (but not univocal) of an anhydrous environment (Burnett and Hall, 1992).

ACKNOWLEDGMENTS

Electronic Supplementary Materials: Supplementary materials are available in the online version of this article at https://doi.org/10.1007/s12583-020-1094-3, (i) the LA-ICPMS and μXRD experimental conditions (ESM I, Table S1); (ii) conodont elements chemical analyses (ESM I, Table S2); (iii) cross-plots showing additional relationships between HFSE (ESM II, Figs. S1–S8).

REFERENCES CITED

Armstrong, H. A., Pearson, D. G., Griselin, M., 2001. Thermal Effects on Rare Earth Element and Strontium Isotope Chemistry in Single Conodont Elements. *Geochimica et Cosmochimica Acta*, 65(3): 435–441. https://doi.org/10.1016/s0016-7037(00)00548-2

Bergström, S. M., Ferretti, A., 2015. Conodonts in the Upper Ordovician Keisley Limestone of Northern England: Taxonomy, Biostratigraphical Significance and Biogeographical Relationships. *Papers in Palaeontology*, 1(1): 1–32. https://doi.org/10.1002/spp2.1003

Bright, C. A., Cruse, A. M., Lyons, T. W., et al., 2009. Seawater Rare-Earth Element Patterns Preserved in Apatite of Pennsylvanian Conodonts?. *Geochimica et Cosmochimica Acta*, 73(6): 1609–1624. https://doi.org/10.1016/j.gca.2008.12.014

Brigatti, M. F., Malferrari, D., Medici, L., et al., 2004. Crystal Chemistry of Apatites from the Tapira Carbonatite Complex, Brazil. *European Journal of Mineralogy*, 16(4): 677–685. https://doi.org/10.1127/0935-1221/2004/0016-0677

Burnett, R. D., Hall, J. C., 1992. Significance of Ultrastructural Features in Etched Conodonts. *Journal of Paleontology*, 66(2): 266–276. https://doi.org/10.1017/s0022336000033783

Chen, J. B., Algeo, T. J., Zhao, L. S., et al., 2015. Diagenetic Uptake of Rare Earth Elements by Bioapatite, with an Example from Lower Triassic Conodonts of South China. *Earth-Science Reviews*, 149: 181–202. https://doi.org/10.1016/j.earscirev.2015.01.013

Collins, M. J., Nielsen-Marsh, C. M., Hiller, J., et al., 2002. The Survival of Organic Matter in Bone: A Review. *Archaeometry*, 44(3): 383–394. https://doi.org/10.1111/1475-4754.t01-1-00071

Cruse, A. M., Lyons, T. W., 2000. Sedimentology and Geochemistry of the Hushpuckney and Upper Tackett Shales Cyclothem Models Revisited. In: Johnson, K. S., ed., Marine Clastics in the Southern Midcontinent, 1997 Symposium. *Oklahoma Geological Survey Circular*, 103: 185–194

Del Moral, B., Sarmiento, G. N., 2008. Conodontos del Katiense (Ordovicico Superior) del Sector Meridional de la Zone Centroibérica (España). *Revista de Micropaleontologia*, 40: 169–245

Dzik, J., 1999. Evolution of Late Ordovician High-Latitude Conodonts and Dating of Gondwana Glaciations. *Bollettino della Società Paleontologica Italiana*, 37(2): 237–253

Dzik, J., 2020. Ordovician Conodonts and the Tornquist Lineament. *Palaeogeography, Palaeoclimatology, Palaeoecology*, 549: 109157. https://doi.org/10.1016/j.palaeo.2019.04.013

Ferretti, A., Bancroft, A. M., Repetski, J. E., 2020a. GECkO: Global Events Impacting Conodont Evolution. *Palaeogeography, Palaeoclimatology, Palaeoecology*, 549: 109677. https://doi.org/10.1016/j.palaeo.2020.109677

Ferretti, A., Malferrari, D., Savioli, M., et al., 2020b. 'Conodont Pearls' do not Belong to Conodonts. *Lethaia*. https://doi.org/10.1111/let.12403

Ferretti, A., Barnes, C. R., 1997. Upper Ordovician Conodonts from the Kalkbank Limestone of Thuringia, Germany. *Palaeontology*, 40(1): 15–42

Ferretti, A., Bergström, S. M., Barnes, C. R., 2014a. Katian (Upper Ordovician) Conodonts from Wales. *Palaeontology*, 57(4): 801–831. https://doi.org/10.1111/pala.12089

Ferretti, A., Bergström, S. M., Sevastopulo, G. D., 2014b. Katian Conodonts from the Portrane Limestone: The First Ordovician Conodont Fauna Described from Ireland. *Bollettino della Società Paleontologica Italiana*, 53(2): 105–119

Ferretti, A., Messori, A., Bergström, S. M., 2014c. Composition and Significance of the Katian (Upper Ordovician) Conodont Fauna of the Vaux Limestone ('Calcaire des Vaux') in Normandy, France. *Estonian Journal of Earth Sciences*, 63(4): 214–219. https://doi.org/10.3176/earth.2014.21

Ferretti, A., Malferrari, D., Medici, L., et al., 2017. Diagenesis does not Invent anything New: Precise Replication of Conodont Structures by Secondary Apatite. *Scientific Reports*, 7(1): 1624. https://doi.org/10.1038/s41598-017-01694-4

Ferretti, A., Schönlaub, H. P., 2001. New Conodont Faunas from the Late Ordovician of the Central Carnic Alps, Austria. *Bollettino della Società Paleontologica Italiana*, 40(1): 3–15

Ferretti, A., Serpagli, E., 1991. First Record of Ordovician Conodonts from Southwestern Sardinia. *Rivista Italiana di Paleontologia e Stratigrafia*, 97(1): 27–34

Ferretti, A., Serpagli, E., 1999. Late Ordovician Conodont Faunas from Southern Sardinia, Italy: Biostratigraphic and Paleogeographic Implications. *Bollettino della Società Paleontologica Italiana*, 37(2/3): 215–236

Frank-Kamenetskaya, O. V., Rozhdestvenskaya, I. V., Rosseeva, E. V., et al., 2014. Refinement of Apatite Atomic Structure of Albid Tissue of Late Devon Conodont. *Crystallography Reports*, 59(1): 41–47. https://doi.org/10.1134/s1063774514010039

Girard, C., Albarède, F., 1996. Trace Elements in Conodont Phosphates from the Frasnian/Famennian Boundary. *Palaeogeography, Palaeoclimatology, Palaeoecology*, 126(1/2): 195–209. https://doi.org/10.1016/s0031-0182(96)00114-9

Grandjean-Lécuyer, P., Feist, R., Albarède, F., 1993. Rare Earth Elements in Old Biogenic Apatites. *Geochimica et Cosmochimica Acta*, 57(11): 2507–2514. https://doi.org/10.1016/0016-7037(93)90413-q

Grandjean, P., Cappetta, H., Michard, A., et al., 1987. The Assessment of REE Patterns and ^{143}Nd/^{144}Nd Ratios in Fish Remains. *Earth and Planetary Science Letters*, 84(2/3): 181–196. https://doi.org/10.1016/0012-821x(87)90084-7

Heckel, P. H., Baesemann, J. F., 1975. Environmental Interpretation of Conodont Distribution in Upper Pennsylvanian (Missourian) Megacy-

clothems in Eastern Kansas. *AAPG Bulletin*, 59: 486–509. https://doi.org/10.1306/83d91cb8-16c7-11d7-8645000102c1865d

Henningsmoen, G., 1948. The Tretaspis Series of the Kullatorp Core. In: Waern, B., Thorslund, P., Henningsmoen, G., eds., Deep Boring through Ordovician and Silurian Strata at Kinnekulle, Vestergötland. *Bulletin of the Geological Institution of the University of Uppsala*, 32: 374–432

Herwartz, D., Tütken, T., Jochum, K. P., et al., 2013. Rare Earth Element Systematics of Fossil Bone Revealed by LA-ICPMS Analysis. *Geochimica et Cosmochimica Acta*, 103: 161–183. https://doi.org/10.1016/j.gca.2012.10.038

Herwartz, D., Tütken, T., Münker, C., et al., 2011. Timescales and Mechanisms of REE and Hf Uptake in Fossil Bones. *Geochimica et Cosmochimica Acta*, 75(1): 82–105. https://doi.org/10.1016/j.gca.2010.09.036

Holmden, C., Creaser, R. A., Muehlenbachs, K., et al., 1996. Isotopic and Elemental Systematics of Sr and Nd in 454 Ma Biogenic Apatites: Implications for Paleoseawater Studies. *Earth and Planetary Science Letters*, 142(3/4): 425–437. https://doi.org/10.1016/0012-821x(96)00119-7

Holser, W. T., 1997. Evaluation of the Application of Rare-Earth Elements to Paleoceanography. *Palaeogeography, Palaeoclimatology, Palaeoecology*, 132(1/2/3/4): 309–323. https://doi.org/10.1016/s0031-0182(97)00069-2

Keenan, S. W., 2016. From Bone to Fossil: A Review of the Diagenesis of Bioapatite. *American Mineralogist*, 101(9): 1943–1951. https://doi.org/10.2138/am-2016-5737

Keenan, S. W., Engel, A. S., 2017. Early Diagenesis and Recrystallization of Bone. *Geochimica et Cosmochimica Acta*, 196: 209–223. https://doi.org/10.1016/j.gca.2016.09.033

Kim, J.-H., Torres, M. E., Haley, B. A., et al., 2012. The Effect of Diagenesis and Fluid Migration on Rare Earth Element Distribution in Pore Fluids of the Northern Cascadia Accretionary Margin. *Chemical Geology*, 291: 152–165. https://doi.org/10.1016/j.chemgeo.2011.10.010

Knüpfer, J., 1967. Zur Fauna und Biostratigraphie des Ordoviziums (Gräfenthaler Schichten) in Thüringen. *Freiberger Forschungshefte*, C220: 1–119

Kocsis, L., Trueman, C. N., Palmer, M. R., 2010. Protracted Diagenetic Alteration of REE Contents in Fossil Bioapatites: Direct Evidence from Lu-Hf Isotope Systematics. *Geochimica et Cosmochimica Acta*, 74(21): 6077–6092. https://doi.org/10.1016/j.gca.2010.08.007

Kohn, M. J., Moses, R. J., 2013. Trace Element Diffusivities in Bone Rule out Simple Diffusive Uptake during Fossilization but Explain *in vivo* Uptake and Release. *Proceedings of the National Academy of Sciences*, 110(2): 419–424. https://doi.org/10.1073/pnas.1209513110

Kowal-Linka, M., Jochum, K. P., Surmik, D., 2014. LA-ICP-MS Analysis of Rare Earth Elements in Marine Reptile Bones from the Middle Triassic Bonebed (Upper Silesia, S Poland): Impact of Long-Lasting Diagenesis, and Factors Controlling the Uptake. *Chemical Geology*, 363: 213–228. https://doi.org/10.1016/j.chemgeo.2013.10.038

Lécuyer, C., Reynard, B., Grandjean, P., 2004. Rare Earth Element Evolution of Phanerozoic Seawater Recorded in Biogenic Apatites. *Chemical Geology*, 204(1/2): 63–102. https://doi.org/10.1016/j.chemgeo.2003.11.003

LeGeros, R. Z., 1981. Apatites in Biological Systems. *Progress in Crystal Growth and Characterization* 4(1/2): 1–45

Li, Y., Zhao, L. S., Chen, Z.-Q., et al., 2017. Oceanic Environmental Changes on a Shallow Carbonate Platform (Yangou, Jiangxi Province, South China) during the Permian-Triassic Transition: Evidence from Rare Earth Elements in Conodont Bioapatite. *Palaeogeography, Palaeoclimatology, Palaeoecology*, 486: 6–16. https://doi.org/10.1016/j.palaeo.2017.02.035

Liao, J. L., Sun, X. M., Li, D. F., et al., 2019. New Insights into Nanostructure and Geochemistry of Bioapatite in REE-Rich Deep-Sea Sediments: LA-ICP-MS, TEM, and Z-Contrast Imaging Studies. *Chemical Geol-*

ogy, 512: 58–68. https://doi.org/10.1016/j.chemgeo.2019.02.039

Lindström, M., Pelhate, A., 1971. Présence de Conodontes dans les Calcaires de Rosan (Ordovicien moyen a Supérieur, Massif Armoricain). Colloque Ordovicien–Silurien, Brest 1971. *Mémoire du Bureau de Recherches Géologiques et Minières*, 73: 89–91

Malferrari, D., Ferretti, A., Mascia, M. T., et al., 2019. How much can We Trust Major Element Quantification in Bioapatite Investigation?. *ACS Omega*, 4(18): 17814–17822. https://doi.org/10.1021/acsomega.9b02426

Martin, E. E., Scher, H. D., 2004. Preservation of Seawater Sr and Nd Isotopes in Fossil Fish Teeth: Bad News and Good News. *Earth and Planetary Science Letters*, 220(1/2): 25–39. https://doi.org/10.1016/s0012-821x(04)00030-5

McArthur, J. M., Walsh, J. N., 1984. Rare-Earth Geochemistry of Phosphorites. *Chemical Geology*, 47(3/4): 191–220. https://doi.org/10.1016/0009-2541(84)90126-8

McLennan, S. M., 2001. Relationships between the Trace Element Composition of Sedimentary Rocks and Upper Continental Crust. *Geochemistry, Geophysics, Geosystems*, 2(4). https://doi.org/10.1029/2000gc000109

Medici, L., Malferrari, D., Savioli, M., et al., 2020. Mineralogy and Crystallization Patterns in Conodont Bioapatite from First Occurrence (Cambrian) to Extinction (end-Triassic). *Palaeogeography, Palaeoclimatology, Palaeoecology*, 549: 109098. https://doi.org/10.1016/j.palaeo.2019.02.024

Nardelli, M. P., Malferrari, D., Ferretti, A., et al., 2016. Zinc Incorporation in the Miliolid Foraminifer *Pseudotriloculina rotunda* under Laboratory Conditions. *Marine Micropaleontology*, 126: 42–49. https://doi.org/10.1016/j.marmicro.2016.06.001

Nothdurft, L. D., Webb, G. E., Kamber, B. S., 2004. Rare Earth Element Geochemistry of Late Devonian Reefal Carbonates, Canning Basin, Western Australia: Confirmation of a Seawater REE Proxy in Ancient Limestones. *Geochimica et Cosmochimica Acta*, 68(2): 263–283. https://doi.org/10.1016/s0016-7037(03)00422-8

Nozaki, Y., Zhang, J., Amakawa, H., 1997. The Fractionation between Y and Ho in the Marine Environment. *Earth and Planetary Science Letters*, 148(1/2): 329–340. https://doi.org/10.1016/s0012-821x(97)00034-4

Paris, F., Pelhate, A., Weyant, M., 1981. Conodontes ashgilliens dans la Formation de Rosan, coupe de Lostmarc'h (Finistère, Massif Armoricain). Conséquences Paléogéographiques. *Bulletin de la Société Géologique et Mineralogique de Bretagne*, 13(2): 15–35

Pattan, J. N., Pearce, N. J. G., Mislankar, P. G., 2005. Constraints in Using Cerium-Anomaly of Bulk Sediments as an Indicator of Paleo Bottom Water Redox Environment: A Case Study from the Central Indian Ocean Basin. *Chemical Geology*, 221(3/4): 260–278. https://doi.org/10.1016/j.chemgeo.2005.06.009

Peppe, D. J., Reiners, P. W., 2007. Conodont (U-Th)/He Thermochronology: Initial Results, Potential, and Problems. *Earth and Planetary Science Letters*, 258(3/4): 569–580. https://doi.org/10.1016/j.epsl.2007.04.022

Person, A., Bocherens, H., Saliège, J. F., et al., 1995. Early Diagenetic Evolution of Bone Phosphate: An X-Ray Diffractometry Analysis. *Journal of Archaeological Science*, 22(2): 211–221. https://doi.org/10.1006/jasc.1995.0023

Picard, S., Lécuyer, C., Barrat, J. A., et al., 2002. Rare Earth Element Contents of Jurassic Fish and Reptile Teeth and Their Potential Relation to Seawater Composition (Anglo-Paris Basin, France and England). *Chemical Geology*, 186(1/2): 1–16. https://doi.org/10.1016/s0009-2541(01)00424-7

Pietsch, C., Bottjer, D. J., 2010. Comparison of Changes in Ocean Chemistry in the Early Triassic with Trends in Diversity and Ecology. *Journal of Earth Science*, 21(S1): 147–150. https://doi.org/10.1007/s12583-010-0195-9

Pucéat, E., Reynard, B., Lécuyer, C., 2004. Can Crystallinity be Used to Determine the Degree of Chemical Alteration of Biogenic Apatites?. *Chemical Geology*, 205(1/2): 83–97. https://doi.org/10.1016/j.chemgeo.2003.12.014

Reynard, B., Lécuyer, C., Grandjean, P., 1999. Crystal-Chemical Controls on Rare-Earth Element Concentrations in Fossil Biogenic Apatites and Implications for Paleoenvironmental Reconstructions. *Chemical Geology*, 155(3/4): 233–241. https://doi.org/10.1016/s0009-2541(98)00169-7

Sanz-López, J., Blanco-Ferrera, S., 2012. Overgrowths of Large Authigenic Apatite Crystals on the Surface of Conodonts from Cantabrian Limestones (Spain). *Facies*, 58(4): 707–726. https://doi.org/10.1007/s10347-012-0295-3

Shen, J., Algeo, T. J., Zhou, L., et al., 2012. Volcanic Perturbations of the Marine Environment in South China Preceding the Latest Permian Mass Extinction and Their Biotic Effects. *Geobiology*, 10(1): 82–103. https://doi.org/10.1111/j.1472-4669.2011.00306.x

Shields, G., Stille, P., 2001. Diagenetic Constraints on the Use of Cerium Anomalies as Palaeoseawater Redox Proxies: An Isotopic and REE Study of Cambrian Phosphorites. *Chemical Geology*, 175(1/2): 29–48. https://doi.org/10.1016/s0009-2541(00)00362-4

Shields, G., Webb, G. E., 2004. Has the REE Composition of Seawater Changed over Geological Time?. *Chemical Geology*, 204: 103–107. https://doi.org/10.1016/j.chemgeo.2003.09.010

Sholkovitz, E., Shen, G. T., 1995. The Incorporation of Rare Earth Elements in Modern Coral. *Geochimica et Cosmochimica Acta*, 59(13): 2749–2756. https://doi.org/10.1016/0016-7037(95)00170-5

Smith, C. I., Craig, O. E., Prigodich, R. V., et al., 2005. Diagenesis and Survival of Osteocalcin in Archaeological Bone. *Journal of Archaeological Science*, 32(1): 105–113. https://doi.org/10.1016/j.jas.2004.07.003

Song, H. J., Wignall, P. B., Song, H. Y., et al., 2019. Seawater Temperature and Dissolved Oxygen over the Past 500 Million Years. *Journal of Earth Science*, 30(2): 236–243. https://doi.org/10.1007/s12583-018-1002-2

Sweet, W. C., Bergström, S. M., 1984. Conodont Provinces and Biofacies of the Late Ordovician. In: Clark, D. L., ed., Conodont Biofacies and Provincialism. *Geological Society of America Special Paper*, 196: 69–87

Sweet, W. C., Donoghue, P. C. J., 2001. Conodonts: Past, Present, Future. *Journal of Paleontology*, 75(6): 1174–1184. https://doi.org/10.1017/s0022336000017224

Toyoda, K., Tokonami, M., 1990. Diffusion of Rare-Earth Elements in Fish Teeth from Deep-Sea Sediments. *Nature*, 345: 607–609. https://doi.org/10.1038/345607a0

Trotter, J. A., Barnes, C. R., McCracken, A. D., 2016. Rare Earth Elements in Conodont Apatite: Seawater or Pore-Water Signatures?. *Palaeogeography, Palaeoclimatology, Palaeoecology*, 462: 92–100. https://doi.org/10.1016/j.palaeo.2016.09.007

Trotter, J. A., Eggins, S. M., 2006. Chemical Systematics of Conodont Apatite Determined by Laser Ablation ICPMS. *Chemical Geology*, 233(3/4): 196–216. https://doi.org/10.1016/j.chemgeo.2006.03.004

Trotter, J. A., Gerald, J. D. F., Kokkonen, H., et al., 2007. New Insights into the Ultrastructure, Permeability, and Integrity of Conodont Apatite Determined by Transmission Electron Microscopy. *Lethaia*, 40(2): 97–110. https://doi.org/10.1111/j.1502-3931.2007.00024.x

Trueman, C. N., Privat, K., Field, J., 2008. Why do Crystallinity Values Fail to Predict the Extent of Diagenetic Alteration of Bone Mineral? *Palaeogeography, Palaeoclimatology, Palaeoecology*, 266(3/4): 160–167. https://doi.org/10.1016/j.palaeo.2008.03.038

Trueman, C. N., Tuross, N., 2002. Trace Elements in Recent and Fossil Bone. In: Kohn, M. J., Rakovan, J., Hughes, J. M., eds., Phosphates: Geochemical, Geobiological and Materials Importance. *Review in Mineralogy and Geochemistry*, 48: 489–521

Vidal, M., Dabard, M.-P., Gourvennec, R., et al., 2011. Le Palèozoïque de la Presqu'Île de Crozon, Massif Armoricain (France). *Gèologie de la France*, 1: 3–45

Webb, G. E., Kamber, B. S., 2000. Rare Earth Elements in Holocene Reefal Microbialites: A New Shallow Seawater Proxy. *Geochimica et Cosmochimica Acta*, 64(9): 1557–1565. https://doi.org/10.1016/s0016-7037(99)00400-7

Webb, G. E., Nothdurft, L. D., Kamber, B. S., et al., 2009. Rare Earth Element Geochemistry of Scleractinian Coral Skeleton during Meteoric Diagenesis: A Sequence through Neomorphism of Aragonite to Calcite. *Sedimentology*, 56(5): 1433–1463. https://doi.org/10.1111/j.1365-3091.2008.01041.x

Wenzel, B., Lécuyer, C., Joachimski, M. M., 2000. Comparing Oxygen Isotope Records of Silurian Calcite and Phosphate—δ^{18}O Compositions of Brachiopods and Conodonts. *Geochimica et Cosmochimica Acta*, 64(11): 1859–1872. https://doi.org/10.1016/s0016-7037(00)00337-9

Weyant, M., Dorè, F., Le Gall, J., et al., 1977. Un épisode Calcaire ashgillien dans l'est du Massif Armoricain: Incidence Sur l'âge des Dépôts Glacio-Marins fini-Ordoviciens. *Comptes Rendus de l'Académie des Sciences*, 284(D): 1147–1149

Wheeley, J. R., Smith, M. P., Boomer, I., 2012. Oxygen Isotope Variability in Conodonts: Implications for Reconstructing Palaeozoic Palaeoclimates and Palaeoceanography. *Journal of the Geological Society*, 169(3): 239–250. https://doi.org/10.1144/0016-76492011-048

Wright, J., Schrader, H., Holser, W. T., 1987. Paleoredox Variations in Ancient Oceans Recorded by Rare Earth Elements in Fossil Apatite. *Geochimica et Cosmochimica Acta*, 51(3): 631–644. https://doi.org/10.1016/0016-7037(87)90075-5

Wright, J., Colling, A., 1995. Seawater: Its Composition, Properties and Behavior. Second ed. Pergamon, Oxford. 168

Wright, J., Seymour, R. S., Shaw, H. F., 1984. REE and Nd Isotopes in Conodont Apatite: Variations with Geological Age and Depositional Environment. In: Clark, D. L., ed., Conodont Biofacies and Provincialism. *Geological Society of America Special Paper*, 196: 325–340

Xin, H., Jiang, S. Y., Yang, J. H., et al., 2016. Rare Earth Element Geochemistry of Phosphatic Rocks in Neoproterozoic Ediacaran Doushantuo Formation in Hushan Section from the Yangtze Gorges Area, South China. *Journal of Earth Science*, 27(2): 204–210. https://doi.org/10.1007/s12583-015-0653-5

Zhang, L., Algeo, T. J., Cao, L., et al., 2016. Diagenetic Uptake of Rare Earth Elements by Conodont Apatite. *Palaeogeography, Palaeoclimatology, Palaeoecology*, 458: 176–197. https://doi.org/10.1016/j.palaeo.2015.10.049

Zhang, L., Cao, L., Zhao, L. S., et al., 2017. Raman Spectral, Elemental, Crystallinity, and Oxygen-Isotope Variations in Conodont Apatite during Diagenesis. *Geochimica et Cosmochimica Acta*, 210: 184–207. https://doi.org/10.1016/j.gca.2017.04.036

Zhang, J., Nozaki, Y., 1996. Rare Earth Elements and Yttrium in Seawater: ICP-MS Determinations in the East Caroline, Coral Sea, and South Fiji Basins of the Western South Pacific Ocean. *Geochimica et Cosmochimica Acta*, 60(23): 4631–4644. https://doi.org/10.1016/s0016-7037(96)00276-1

Zhang, J., Amakawa, H., Nozaki, Y., 1994. The Comparative Behaviors of Yttrium and Lanthanides in the Seawater of the North Pacific. *Geophysical Research Letters*, 21(24): 2677–2680. https://doi.org/10.1029/94gl02404

Zhao, L. S., Chen, Z.-Q., Algeo, T. J., et al., 2013. Rare-Earth Element Patterns in Conodont Albid Crowns: Evidence for Massive Inputs of Volcanic Ash during the Latest Permian Biocrisis?. *Global and Planetary Change*, 105: 135–151. https://doi.org/10.1016/j.gloplacha.2012.09.001

Žigaitė, Ž., Qvarnström, M., Bancroft, A., et al., 2020. Trace and Rare Earth Element Compositions of Silurian Conodonts from the Vesiku Bone Bed: Histological and Palaeoenvironmental Implications. *Palaeogeography, Palaeoclimatology, Palaeoecology*, 549: 109449. https://doi.org/10.1016/j.palaeo.2019.109449